Increasing the Photon Energy for Photonuclear Experiments in MAX-lab by Phase Modulating the SLED Pulse

Olsson, David; Lilja, Per; Malmgren, Lars

2016

CODEN:LUTEDX/(TEAT-7242)/1-11/(2016)

Increasing the Photon Energy for Photonuclear Experiments in MAX-lab by Phase Modulating the SLED Pulse

David Olsson, Per Lilja, and Lars Malmgren

Electromagnetic Theory
Department of Electrical and Information Technology
Lund University
Sweden

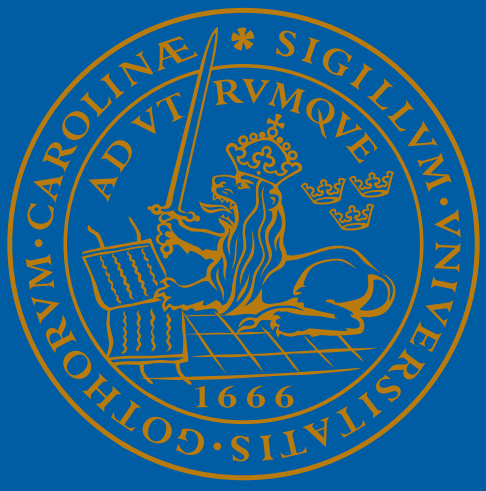

(TEAT-7242)/1-11/(2016): D. Olsson, *etal*, Increasing the Photon Energy for Photonuclear Experiments in MAX-lab

David Olsson
david.olsson@maxiv.lu.se

MAX IV Laboratory
Lund University
P.O. Box 118
SE-221 00 Lund
Sweden

Per Lilja
per.lilja@maxiv.lu.se

MAX IV Laboratory
Lund University
P.O. Box 118
SE-221 00 Lund
Sweden

Lars Malmgren
per.lilja@maxiv.lu.se

MAX IV Laboratory
Lund University
P.O. Box 118
SE-221 00 Lund
Sweden

Editor: Mats Gustafsson

Abstract

The nuclear physics facility at MAX-lab requires high energy electrons for photonuclear experiments. These electrons are first accelerated in two LINACs that are fed via a SLED system. Arcing in the waveguide structures is currently the limiting factor of the available electron energy. In this report, the implementation of a phase modulation scheme into the injector system is presented. This makes it possible to increase the power delivered to the LINACs and thereby increasing the energy gain without increasing the risk of arcing. Calculations of the available electron energy at the nuclear physics facility using focal plane detectors and tracking code is also presented.

1 Motivation

The MAX-lab injector which is used for injection into the storage rings has undergone an energy upgrade from 100 MeV racetrack microtron to two LINAC structures equipped with SLED cavities. A new tagger spectrometer for photonuclear experiments was donated to MAX-lab by Saskatchewan Accelerator Laboratory (SAL) [5]. The two LINAC structures were initially designed to operate at an energy gain of 125 MeV each, but are currently operating at a gain of 100 MeV each due to risk of arcing. Arcing in a waveguide structure is a result of breakdowns of the electric field, and one way to avoid this is to decrease the peak electric field of the incoming RF pulse. In a SLED system, this can be achieved by phase modulating the RF pulse, while the energy gain is kept at almost the same level. A goal is to increase the electron energy since it would make it possible to produce tagged photons with an energy of 200 MeV and thereby to study the pion photoproduction near threshold.

A second goal is to calculate the electron energy delivered to the nuclear physics facility. Today, the energy is estimated from the current delivered to an upstream located magnet which gives a higher value since some energy is lost as dipole radiation in MAX I and in the transport.

2 Photonuclear Experiments at MAX-lab

The electrons are generated in a 3-cell thermionic RF gun and accelerated in two constant-gradient traveling wave LINACs with an energy gain of 100 MeV each. During ring injections, the electron beam is recirculated through the two LINACs giving a total energy of 400 MeV. However, the beam is not recirculated when running nuclear physics experiments. Thus, the total electron energy is 200 MeV. The injector was initially designed for a maximum energy gain of 125 MeV per LINAC, but this gain has never been reached because of arcing. Each LINAC is fed by a klystron via a SLED system which can be seen in Figure 1 together with the rest of the injector [1]. After acceleration, the electrons are injected into the MAX I storage ring which is used as pulse stretcher during tagged photon experiments. MAX I is filled at a repetition frequency of 10 Hz, and the stored beam is then

slowly extracted when the beam energy decreases. The extracted electron beam is then passed through an achromatic beam line to the tagger spectrometers.

The tagger system consists of two tagger spectrometers, the End Point Tagger (ET) and the Main Tagger (MT). These consist of a radiator made of thin aluminium foil where a small portion of the electrons will produce photons by the bremsstrahlung process. The energy of the electrons that have produced photons is then measured in a spectrometer consisting of a bending magnet and a focal plane. In the focal plane, an array of scintillation detectors are located with which the electron curvature radius is determined and hence their energy. The incoming electron beam energy at the radiator is given by the dipole field in one of the bending magnets in the achromatic beam line. The bremsstrahlung photon energy is then determined as the difference of the electron energy before and after the radiator. Figure 2 shows the tagger system.

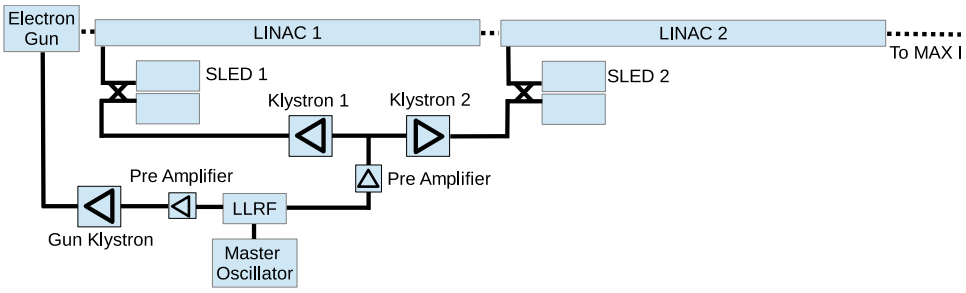

Figure 1: The MAX-lab injector.

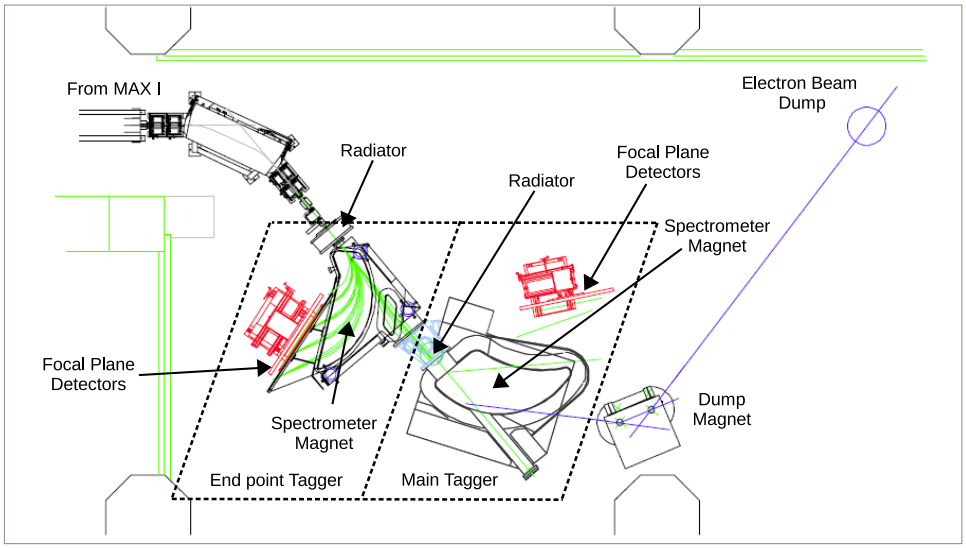

Figure 2: The nuclear physics tagger system.

3 Phase Modulating the SLED Pulse

The SLAC Energy Development (SLED) is a passive pulse compression network that has been used in electron accelerator facilities since the 70's. The network consists of two normal conducting pillbox cavities that are combined by a 3 dB $\pi/2$ hybrid waveguide coupler. The two cavities are identical, and the MAX-lab design is constructed so that the TE_{015} mode is the mode of operation. The fields of the TE_{015} mode are

$$\begin{cases} \boldsymbol{E}(\rho,\phi,z) = -A\eta_0\sqrt{\left(\frac{j'_{0,1}}{a}\right)^2+\left(\frac{5\pi}{L}\right)^2}J'_0\left(\frac{j'_{0,1}}{a}\rho\right)\sin\left(\frac{5\pi}{L}z\right)\hat{\boldsymbol{\phi}} \\ \boldsymbol{H}(\rho,\phi,z) = \frac{5A\pi}{L}J'_0\left(\frac{j'_{0,1}}{a}\rho\right)\cos\left(\frac{5\pi}{L}z\right)\hat{\boldsymbol{\rho}} + \frac{Aj'_{0,1}}{a}J_0\left(\frac{j'_{0,1}}{a}\rho\right)\sin\left(\frac{5\pi}{L}z\right)\hat{\boldsymbol{z}} \end{cases} \tag{3.1}$$

where A is a constant, η_0 the impedance of free space, $J_0(x)$ is the Bessel function of index 0 and $J'_0(x)$ its derivative, $j'_{0,1} \approx 3.83$ the first zero of $J'_0(x)$, a the cavity radius, and L the cavity length. The reason for using this mode is that it has a quite high Q factor, and there are no currents in the regions where the lateral body is welded to the top and bottom parts (in contrary to the fundamental TM_{010} mode). As seen in (3.1), $\boldsymbol{J}(a,\phi,0) = \boldsymbol{J}(a,\phi,L) = 0$ since $\boldsymbol{J} = \hat{\boldsymbol{n}} \times \boldsymbol{H}$, where $\boldsymbol{J}$ is the surface current density, and $\hat{\boldsymbol{n}}$ the outgoing normal vector of the cavity surface. Figure 3 shows the field distribution in the cavity obtained from COMSOL Multiphysics, and Figure 4 shows the two cavities with the coupler.

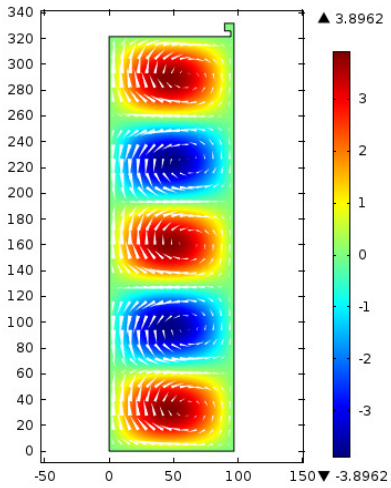

Figure 3: $E_\phi(r,\phi,z)$ (color scale) and $\boldsymbol{H}(r,\phi,z)$ (white cones) of the TE_{015} mode.

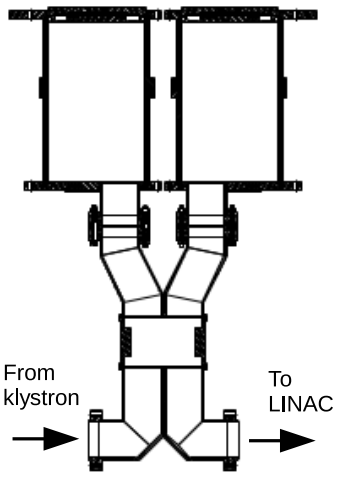

Figure 4: The SLED cavities with the 3dB $\pi/2$ hybrid coupler.

When the power to a heavily overcoupled cavity is abruptly turned off, the cavity will radiate power back to the source which initially has a magnitude that is up to four times the incident source power. The SLED is based on that concept, but instead of having a single resonant cavity that radiates all its emitted power back

to the source, the 3 dB $\pi/2$ hybrid coupler cancels out the emitted power from the two cavities that travels back to the source, and directs it to the load (the LINAC). The emitted electric field from the cavities to the load, E_C can be described by a first order differential equation [3]

$$T_c \frac{E_C}{dt} + E_C = -\alpha E_K \tag{3.2}$$

where $T_c = \frac{2Q_0}{\omega(\beta+1)}$ is the rise time, Q_0 the unloaded Q factor, and β the coupling factor of one of the cavities. E_K is the field delivered by the source, ω the angular frequency, and $\alpha = \frac{2\beta}{\beta+1}$. Note that (3.2) is only valid if both the cavities are fine tuned to the operating frequency [2]. The field delivered to the load, E_L, is the sum of the direct field from the source, E_K, and the field emitted from the cavities, E_C.

$$E_L = E_K + E_C \tag{3.3}$$

Instead of just turning off the power at a certain time t_1, the phase is reversed 180 degrees which makes the direct field and emitted field add in phase at the load. This is how conventional operation of SLED cavities works. If the field from the pulsed source starts at t_0 with amplitude $-E_0$, reversed in phase 180 degrees at t_1, and ends at t_2, then E_K can be written as

$$E_K(t) = -E_0(\theta(t-t_0) - \theta(t-t_1)) + E_0(\theta(t-t_1) - \theta(t-t_2)) \tag{3.4}$$

where $\theta(t)$ is the Heaviside step function. By solving (3.2) and (3.3) for (3.4), E_L can be written as in (3.5). Note that when solving (3.2), E_C must be continous in time.

$$E_L = \begin{cases} -E_0 + \alpha E_0(1 - e^{-\frac{t-t_0}{T_c}}) & , t_0 \leq t \leq t_1 \\ E_0(1-\alpha) + \alpha E_0(2 - e^{-\frac{t_1-t_0}{T_c}})e^{-\frac{t-t_1}{T_c}} & , t_1 < t \leq t_2 \\ \alpha E_0((2 - e^{-\frac{t_1-t_0}{T_c}})e^{-\frac{t_2-t_1}{T_c}} - 1)e^{-\frac{t-t_2}{T_c}} & , t_2 < t \end{cases} \tag{3.5}$$

In conventional SLED operation, the maximum field at the load occur at t_1.

$$(E_L)_{max} = E_L(t_1) = E_0 + \alpha E_0(1 - e^{-\frac{t_1}{T_c}}) \tag{3.6}$$

If the cavities are heavily overcoupled and the charging time is long enough, a voltage gain of a factor close to 3 can be achieved at t_1 which corresponds to a power gain of almost 9. However, this voltage peak is the source of the arcing in the LINACs. Therefore, in order to avoid arcing, and thereby being able to increase the energy gain of the LINACs, the peak field has to be flattened out. One way of doing this is to phase modulate E_K where the phase shift is performed in several smaller steps going from t_1 to t_{N-1} when the phase has been shifted 180 degrees relative to the initial phase, φ_0. A similar system has already been implemented at Elettra [6],[4]. Figure 5 shows E_K in a polar diagram during conventional operation

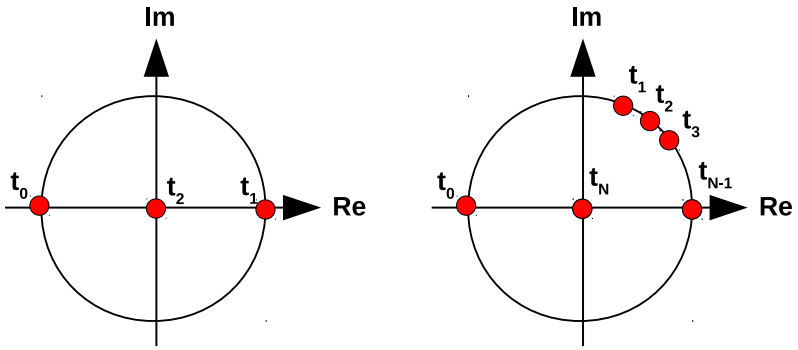

Figure 5: Modulation scheme for conventional operation (a) and phase modulation operation (b).

and during the phase modulation operation described above. With this modulation technique E_K can be written as in (3.7).

$$E_K(t) = E_0 \sum_{n=0}^{N-1} (\theta(t - t_n) - \theta(t - t_{n+1}))e^{j\varphi_n} \tag{3.7}$$

E_L is now a complex vector and can be written as

$$E_L(t) = \begin{cases} -E_0 + \alpha E_0(1 - e^{-\frac{t-t_0}{T_c}}) & , t_0 \leq t \leq t_1 \\ E_0 e^{j\varphi_n}(1-\alpha) + (\alpha E_0 e^{j\varphi_n} - E_0 e^{j\varphi_{n-1}} + E_L(t_n))\, e^{-\frac{t-t_n}{T_c}} & , t_n < t \leq t_{n+1} \\ & , n = 1, 2, .., N \\ E_L(t_N) e^{-\frac{t-t_N}{T_c}} & , t_N < t \end{cases} \tag{3.8}$$

If the modulation scheme is selected so that the peak field has the same level at $t_1, t_2, \ldots, t_{N-1}$ (i.e. if we're keeping the peak field on a flat top when doing the phase shifting), the maximum field obtained in (3.8) is

$$(E_L)_{max} = |E_L(t_1)| = |E_0 e^{j\varphi_1} + \alpha E_0(1 - e^{-\frac{t_1}{T_c}})| \tag{3.9}$$

which is lower than in (3.6) if $\varphi_1 \neq 0$. The SLED cavities in MAX-lab have $Q_0 \approx 100000$, $\beta = 6.2$, and $\omega = 2\pi \cdot 2.9985$ GHz. During conventional operation, the pulse length is 4 μs, and the phase shift occurs at $t_1 = 3.25$ μs (assuming the pulse starts at $t_0 = 0$). As an example, if a phase modulation scheme (see Figure 5) is selected where $[t_0, t_1, \ldots, t_8] = [0, 3.25, 3.30, 3.35, 3.40, 3.45, 3.50, 3.55, 4]\mu$s and $[\varphi_0, \varphi_1, \ldots, \varphi_7] = [180°, 72°, 65°, 57°, 48°, 37°, 24°, 0°]$, the maximum E-field can be lowered to 82% compared to conventional operation. Figure 6 shows $|E_C|$ and $|E_L|$ during conventional and phase modulation operation.

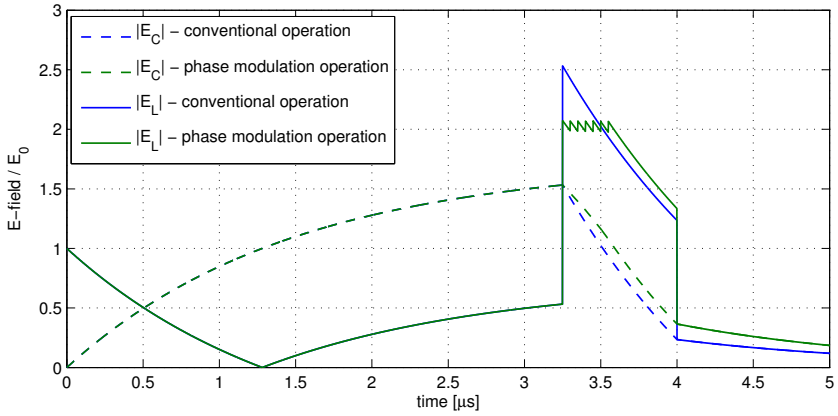

Figure 6: $|E_C|$ and $|E_L|$ during conventional operation (blue), and phase modulation operation (green).

The group velocity $v_g(z)$ of the traveling wave inside a constant-gradient LINAC decreases linearly with the distance z, and the time it takes for the wave to travel from the LINAC input ($z = 0$) to z, $\Delta t(z)$, is given by

$$\Delta t(z) = -\frac{L}{g v_g(0)} \ln\left(1 - g\frac{z}{L}\right) \tag{3.10}$$

where $g = \frac{v_g(0) - v_g(L)}{v_g(0)}$ is the group velocity gradient, and L the length of the LINAC structure. If E_a is the accelerating field along the structure, then $E_a(z,t) = E_a(0, t - \Delta t(z))$ if the beam loading is neglected. The energy gain of an ultrarelativistic electron that enters the LINAC section at t, $\Delta W(t)$, is

$$\Delta W(t) = q\cos(\psi)\int_0^L E_a(0, t - \Delta t(z) + \frac{z}{c_0})\,\mathrm{d}z \tag{3.11}$$

where q is the elementary charge, ψ the phase relative to the crest of the wave, and c_0 the speed of light. Note that if the RF pulse is phase modulated, the bunches along the bunch train will have different phases when exiting the LINAC. This might not be suitable for all applications, but in our case, beam energy is most important. Figure 7 shows $|\Delta W|$ during conventional operation and phase modulation operation when the electrons are on crest. The peak energy gain is almost 1% lower for the latter. Here, $v_g(0) = 0.037c_0$, $v_g(L) = 0.014c_0$, and $L = 5$ m.

4 Experimental set-up

A Low Level RF (LLRF) box with a Micro Controller Unit (MCU), an IQ modulator, and four fast 4-channel multiplexers was used to phase modulate the incoming 3 GHz signal. This box was initially designed as a prototype for the MAX IV LLRF system. However, a simpler and more reliable design with conventional RF switches instead of the MCU and IQ-modulator was chosen, so the prototype was modified for phase

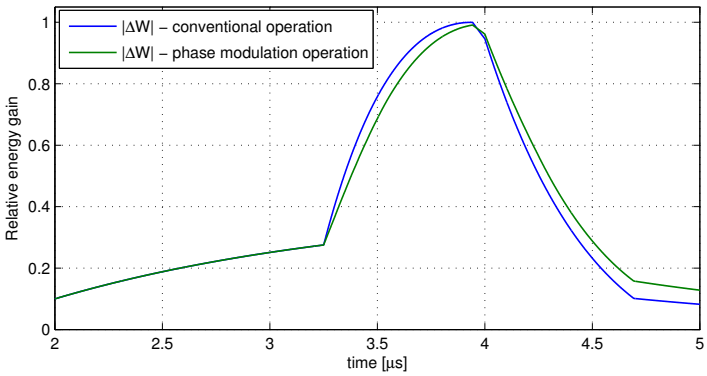

Figure 7: Normalized energy gain for conventional operation (blue), and phase modulation operation (green).

modulation instead. The MCU is a Microchip dsPIC30F4012 that is running at 20 MIPS and is clocked externally by a standard 10 MHz RF instrument signal which allows it to be synchronized with the trigger signals to the injector. The MCU output pins control the four 4-channel multiplexers (Fairchild FST3253). By using them in pair with the output pins connected within the pair, and by only keeping one multiplexer in each pair active at the time, eight independent channels can be used in each pair. Hence, the phase shifting can be done in eight steps which corresponds to $N = 8$ in (3.7). Note that it is the pre amplifier that switches the RF pulse on at t_0 and off at t_N, so the first state is actually active in the LLRF box a time period before t_0, and the $(N-1)$:th state is still active a time period after t_N, thus a state where $E_K = 0$ at t_N is not needed. Each multiplexer pair switches eight analog voltages to the IQ modulator (Analog Devices ADL5374). A user interface consisting of physical buttons and an LCD display makes it possible to adjust the settings in the LLRF box without an external computer. Figure 8 shows a block diagram of the LLRF box. The modulation scheme described in the previous section was used with some minor adjustments to optimize the pulse shape from Klystron 1 since this klystron runs in a mode that allows higher output power compared to Klystron 2. These adjustments were needed since there were some reflections from SLED 1 which affected the output of the klystron after the first phase shift at t_1.

5 Energy Measurements

The MT spectrometer was used during the energy measurement experiments. There exists a 2D magnetic field map of the MT spectrometer magnet with a resolution of 10 mm obtained from previous measurements. This field map was interpolated in steps of 1 mm and imported into MATLAB, where an ODE (Ordinary Differential Equation) tracking program was written. Figure 9 shows the field map with three different electron trajectories diverging from the radiator position. These electrons have the same energy, and they intersect in a focus point at the focal plane which

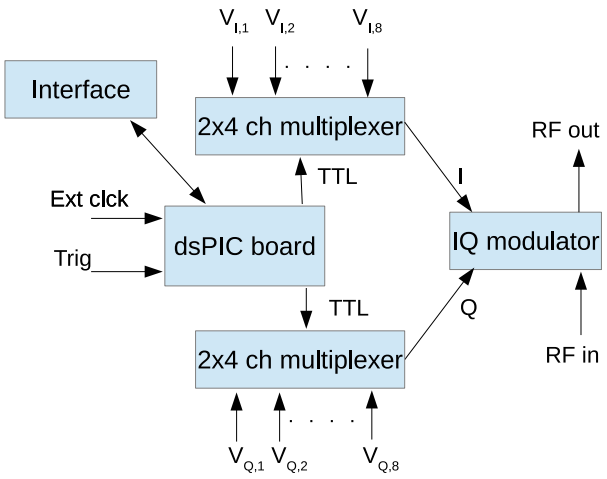

Figure 8: A block diagram showing the LLRF box.

is shown as a green line. Unfortunately, there were only measurement points in the MT field map that could fully cover trajectories that intersect between detector 24 and 51 at the focal plane. A Gauss meter was placed inside the MT magnet so the relative magnetic field could be measured without the error introduced due to hysteresis when the current to the MT magnet was swept. The MT magnet current was swept until the beam hit the focal plane detectors. Then, the energy was calculated from the ODE program using the corresponding magnetic field and trajectory. The measurements started at the energy level, $W_{sept} = 198.2$ MeV, which is the standard safe level during nuclear physics experiments. W_{sept} is the kinetic energy calculated from the currents to one of the dipole magnets in MAX I. The klystron output was then increased, and the measurements were also performed at $W_{sept} = 212.3$ MeV and 221.1 MeV. The number of energy levels was limited to three since it is very time consuming to trim the facility for new energy levels.

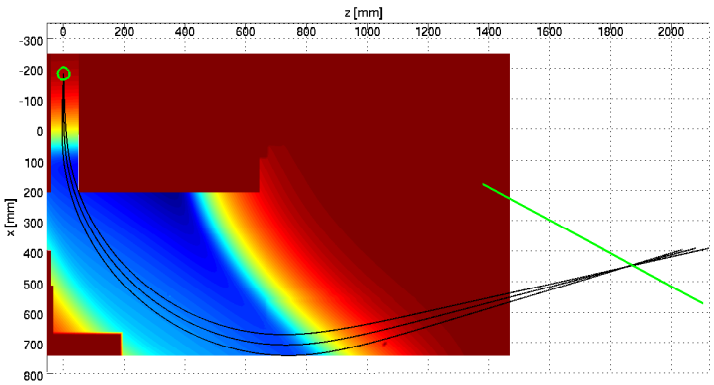

Figure 9: The trajectories of three different electrons (black lines) that are diverging from the radiator position (green circle), and refocusing at the focal plane (green line). The color scale shows the magnitude of the magnetic field.

6 Results

Figure 10 shows the signal delivered to LINAC 1 during conventional operation and phase modulation operation measured by a diode peak detector. The measured pulse shapes show good agreement with the simulations. There are some reflections in the measurement cables that are visible after the pulses have ended. During the test, the output of Klystron 1 could not be increased as much as we hoped due to arcing. However, this arcing was located in SLED 1 (or in its 3dB hybrid coupler), and was therefore not the normal LINAC arcing. As seen in Figure 6, phase modulation does not reduce the risk of arcing in the SLED cavities since $(E_c)_{max}$ is not decreased. There were also frequent interlocks due to current failures in the modulator to Klystron 1 at higher power outputs. Klystron 2 was running stable during the test. The klystrons can deliver higher output power, but we did not go further since there is always a risk of damaging the injector severely when doing this type of experiments.

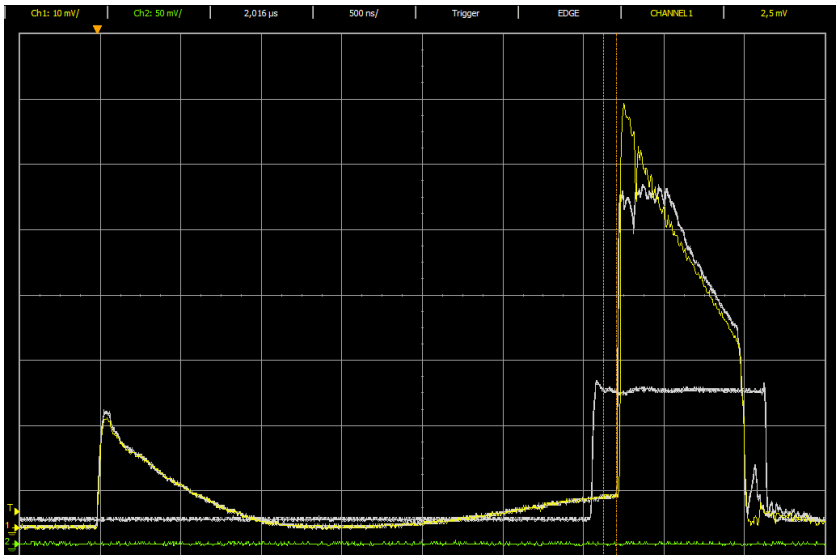

Figure 10: The signal delivered to LINAC 1 during conventional operation and phase modulation operation measured by a directional coupler and a diode peak detector. The rectangular curve is the RF pulse delivered to the electron gun.

Table 1 shows the result of the MT measurements for the three energies. The highest calculated kinetic energy at the MT, W_{MT}, during the phase modulation test was above 204 MeV compared to roughly 183 MeV during normal nuclear physics experiments. This is an energy increase of almost 12%. As seen, W_{sept} is 8.1-8.5% higher compared to W_{MT}. This factor agrees well with the electron beam energy estimated in previous measurements of the lowest energy states of $^{12}\mathbf{C}$.

These experiments were performed in February 2013. After that, more conditioning of the LINACs and SLEDs has been made which has raised the safe level during nuclear physics experiments further.

W_{sept} [MeV]	Detector	W_{MT} [MeV]	W_{sept}/W_{MT}
198.2	49.85	183.4	1.081
198.2	33.05	182.6	1.085
212.3	45.53	196.1	1.083
212.3	36.08	195.6	1.085
212.3	24.21	195.6	1.085
221.1	49.70	204.6	1.081
221.1	41.08	204.3	1.082

Table 1: The measurement results at the focal plane detectors showing the energy calculated from the septum magnet current, intersection point, and the energy calculated in the ODE tracking program.

7 Conclusion

The results show that a phase modulation scheme can be integrated into the MAX-lab injector. This allows the energy gain to be increased without increasing the risk of arcing in the LINAC structures. During the experiments, the highest measured electron energy was above 204 MeV which is an energy increase of 12 % compared to the previous safe level during conventional operation. However, arcing in one of the SLED cavities was the limiting factor to how much the delivered power could be increased. As discussed, implementing a phase modulation scheme does not help if the arcing is located in the SLED. Another problem was frequent interlocks caused by high modulator currents at high power levels. The calculated energy levels using focal plane detectors and tracking code also agree well with previous measurements.

Acknowledgment

The authors would like to thank Kurt Hansen, Lennart Isaksson, and Bent Schröder at the Nuclear Physics department for their help during the experiments. Also big thanks to Robert Nilsson in the RF group for the help with the electronics, and to Anders Karlsson at the Department of Electrical and Information Technology.

References

[1] B. Andersson et al. “The 500 MeV injector for MAX-lab using a recirculated LINAC”. In: *European Particle Accelerator Conference (EPAC)*. 2000, pp. 1687–1689.

[2] A. Chao and M. Tigner. *Handbook of accelerator physics and engineering*. World Scientific Publisher, 2009.

[3] Z. Farcas et al. *SLED: A method of doubling SLAC’s energy*. Tech. rep. SLAC-PUB-1453. Stanford Linear Accelerator Center, 1974.

[4] C. Serpico et al. "Phase-modulation SLED mode at elettra". In: *International Particle Accelerator Conference (IPAC)*. 2011, pp. 83–85.

[5] J. Vogt et al. "The photon tagging facility at the saskatchewan accelerator laboratory". *Nuclear Instruments and Methods in Physics Research* A324 (1993), pp. 198–208.

[6] D. Wang et al. "Phase-modulation SLED mode on BTW sections at Elettra". In: *Particle Accelerator Conference (PAC)*. 2009, pp. 1069–1071.